Curved and Layer. Struct. 2022; 9:396–402 DE GRUYTER

Research Article

Farouk Omar Hamdoon, Alaa Abdulhady Jaber*, and Enass H. Flaieh

An overset mesh approach for a vibrating cylinder in uniform flow

https://doi.org/10.1515/cls-2022-0178
Received May 01, 2022; accepted Aug 18, 2022

Abstract: This paper has numerically investigated two-dimensional laminar flow over a vibrating circular cylinder. Numerical simulation is performed using the dynamic overset mesh method available in commercial software ANSYS FLUENT 19.0. A simple harmonic motion is applied to simulate the cylinder vibration using the user-defined function (UDF) tool in FLUENT. To examine the accuracy and the capability of the present overset mesh approach, two test types of cylinder vibration are simulated: crossflow and inline vibrations. All simulations are performed at a constant Reynolds number (Re = 100) to predict the occurrence of synchronization or lock-in phenomenon. For the case of crossflow vibration, it is observed that lock-in occurs with cylinder oscillation frequency near the Strouhal frequency of the fixed cylinder. However, for the inline vibration, lock-in occurs near twice the Strouhal frequency of the fixed cylinder. Furthermore, in the case of crossflow oscillation, the frequency content in the lift coefficients' time history is successfully linked to the phase portraits' shape and the vorticity field. The simulation results are consistent with the available published data in the literature. This indicates that the present numerical technique is valid and capable of modeling flows with moving structural systems.

Keywords: Cylinder vibration, laminar flow, overset mesh, Fast Fourier transform, crossflow, inline vibration

1 Introduction

The flow problem around oscillating bodies has numerous appeals, both in terms of flow field physics and actual engineering applications. The nonlinear interplay between the body motion and the incident flow produces a variety of intriguing phenomena, including vortex lock-in, hysteresis and bifurcation, modification of vortex shedding patterns, and chaotic wake behavior. From an engineering standpoint, this subject is particularly pertinent to wind engineering, offshore exploration, maritime structures, and nuclear and conventional power plants. One of the main interesting flow phenomena around a vibrating structure is lock-in or synchronization between the vortex shedding and structural vibration frequencies. Even though the cylinder is in a stable condition throughout a given range of Reynolds numbers, a cylinder in a uniform flow causes unsteady flow. For a stationary circular cylinder, unsteady flow is detected as periodic vortex shedding, referred to as the von Kármán vortex street, and the Reynolds number determines the Strouhal frequency of vortex shedding. The cylinder oscillates due to the vortex-induced force acting on it as a result of this periodic vortex shedding. Inherently, a forced oscillating circular cylinder has two frequency components: the applied driving frequency and the Strouhal frequency corresponding to the flow across the circular cylinder. At a particular oscillation state, these two frequency components can cause synchronization . During lock-in, the vortex shedding frequency deviates from the Strouhal shedding frequency of a fixed structure and becomes identical to the frequency of the vibrating structure. Lock-in can amplify the response of the vibrating structure resulting in fatigue failure. Hence, cylindrical structures such as cooling towers, heat exchanger tubes, chimney stacks, nuclear reactor fuel rods, offshore structures, etc., may collapse due to the lock-in phenomenon. Consequently, several strategies have been implimented to control and suppress the effect of vortex induced vibration [1–4].

Numerous experimental and computational studies have been conducted to investigate the flow over a circular cylinder undergoing forced vibrations. Bishop and Hassan [5] conducted experimental work to study how the fluid forces are influenced by forcing a circular cylinder to vibrate in a crossflow (transverse) direction. Under the influence of lock-in, the lift force frequency synchronizes with the vibrating cylinder frequency. Koopmann [6] investigated the flow over a circular cylinder undergoing forced crossflow

***Corresponding Author: Alaa Abdulhady Jaber:** Mechanical Engineering Department, University of Technology- Iraq, Baghdad, Iraq; Email: alaa.a.jaber@uotechnology.edu.iq
Farouk Omar Hamdoon: College of Engineering, University of Wasit , Wasit, Iraq
Enass H. Flaieh: Mechanical Engineering Department, University of Technology- Iraq, Baghdad, Iraq

vibration experimentally. The study focused on obtaining the lock-in boundary. Griffin and Ramberg [7] examined the influence of inline vibrating on the vortex shedding from circular cylinders. The study showed that lock-in, in this case, happened when the inline oscillation of the cylinder approached twice the Strouhal shedding frequency of the fixed cylinder. Comprehensive experimental results and reviews concerning the lock-in phenomenon of vortex shedding from vibrating cylinders were conducted in [8–12]. Furthermore, several numerical studies with a particular focus on the flow around a vibrating cylinder were reported in the literature.

The first successful numerical simulation of flow past a vibrating cylinder was conducted by Hurlbut *et al.* [13] in 1982. The marker and Cell finite difference method was used to investigate three types of cylinder motion: oscillation in a still fluid, inline oscillation, and crossflow oscillation to a moving stream. Nobari and Naredan [14] employed a novel finite element method that uses discretization along the characteristic line. Two types of cylinder motion were considered: inline and crossflow oscillation. The occurrence of lock-in and the bounds of the lock-in region were also investigated in this study. Shen-Wei Su *et al.* [15] presented a new immersed boundary technique to simulate flow interacting with solid boundaries. Four different test cases were studied with this technique (rotating ring flow, lid-driven cavity, flows around a fixed cylinder, and an inline oscillating cylinder) to examine the numerical accuracy of the method. Placzek *et al.* [16] implemented a finite volume method with an industrial CFD code in which a coupling procedure was utilized to obtain the cylinder motion. The simulation was performed for forced and free crossflow oscillations. Moreover, different numerical approaches were conducted by researchers [17–20] to investigate the lock-in of flow over an oscillating cylinder.

The main contribution of the present study is to implement the dynamic overset mesh technique available in the commercial software FLUENT to simulate a circular cylinder vibrating in uniform flow at Reynolds number Re = 100. The objective of this numerical simulation is focused on verifying the capability of this overset mesh feature in identifying the occurrence of the lock-in phenomenon for a cylinder undergoing two cases of forced vibration: cross flow and inline oscillations.

This paper is organized as follows: the following section deals with the mathematical modeling of the considered problem, considering flow and vibration modeling. In Section 3, the computational domain and the mesh analysis are discussed. After that, the validation analysis of the proposed modeling is conducted in Section 4. Then, the obtained results are deliberated in Section 5. Finally, the paper is concluded in Section 6.

2 Mathematical modeling

The model investigated in the present work is a two-dimensional laminar incompressible flow over a circular cylinder undergoing forced vibration. The governing equations consist of the fluid dynamics equations and the structural dynamics equations.

2.1 Flow model

The governing equations for the two-dimensional laminar incompressible flow can be expressed as follows:

Continuity equation:

$$\frac{\partial \rho}{\partial t} + \frac{\partial u}{\partial x} + \frac{\partial v}{\partial y} = 0 \tag{1}$$

Momentum equation:

$$\frac{\partial u}{\partial t} + \frac{\partial u^2}{\partial x} + \frac{\partial (uv)}{\partial y} = -\frac{\partial p}{\partial x} + \frac{1}{Re}\left[\frac{\partial^2 u}{\partial x^2} + \frac{\partial^2 u}{\partial y^2}\right] \tag{2}$$

$$\frac{\partial v}{\partial t} + \frac{\partial (uv)}{\partial x} + \frac{\partial v^2}{\partial y} = -\frac{\partial p}{\partial y} + \frac{1}{Re}\left[\frac{\partial^2 v}{\partial x^2} + \frac{\partial^2 v}{\partial y^2}\right] \tag{3}$$

The velocity components in x- and y-directions are u and v, respectively; p is the pressure; Re is the Reynolds number defined as $Re = \rho UD/\mu$ in which U is the free stream velocity of the fluid, D is the diameter of the cylinder, ρ is density, and μ is the dynamic viscosity of the fluid. The simulation parameters are selected to adopt a constant Reynolds number (Re = 100).

2.2 Vibration model

A simple harmonic motion is applied to define the vibration of the cylinder in crossflow and inline directions, as follows:

$$Y(t) = A_Y \sin(2\pi f_v t) \tag{4}$$

$$X(t) = A_X \sin(2\pi f_v t) \tag{5}$$

Where $Y(t)$ and $X(t)$ are the cylinder motion in crossflow and inline directions, respectively. A_Y and A_X are the vibration amplitudes of the cylinder; f_v is the frequency of the cylinder vibration derived from the excitation ratio, which is $F = f_V/f_S$, where f_S is the Strouhal shedding frequency of the fixed cylinder.

The flow field is solved numerically using ANSYS FLUENT 19.0 based on the Finite Volume Method (FVM). A user-defined function (UDF) is used to simulate the cylinder's vibration motion with FLUENT. Pressure–velocity coupled equations are solved by a COUPLED algorithm. The first-order implicit scheme is used for transient terms. All simulations are performed using time step sizes of Δt = 0.004 s.

3 Computational domain and mesh

The computational domain used in the current simulation is shown in Figure 1. The computational domain extends to 10 D from the cylinder to the inlet of the domain, 25 D behind the cylinder, and 10 D for both upper and lower boundaries, where D is the diameter of the cylinder. The cylinder can vibrate in crossflow and inline directions. No-slip boundary condition is imposed on the cylinder, and the upper and lower boundary conditions are of slip-wall type. The velocity at the inflow boundary is set to be the same as the free stream velocity. The pressure at the outflow boundary is set as a reference value of zero.

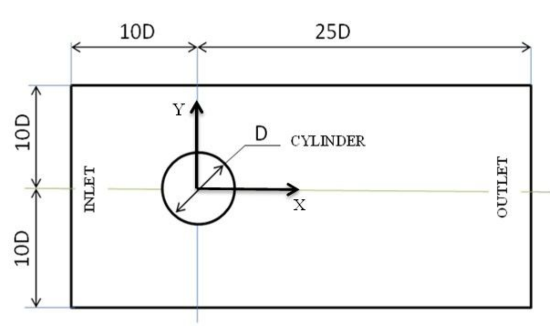

Figure 1: Schematic drawing of the computational domain

Overset mesh method available in ANSYS FLUENT 19.0 is implemented to simulate the flow past the vibrating cylinder. Overset mesh technique combines two overlapping meshes [21, 22]. The first rectangular grid of total cells = 23584 is the static background mesh. The second cylindrical grid of total cells = 6641 is the moving component mesh with an inner diameter of D and an outer diameter of 2.5 D. The moving component mesh is attached to the moving cylinder. Hence, the cylinder moves along the fluid domain without any mesh deformation. Overset background and component meshes are depicted in Figure 2.

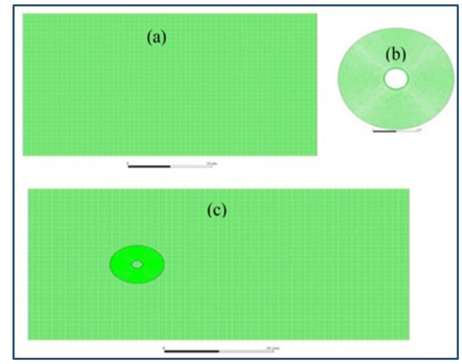

Figure 2: (a) Overset background mesh, (b) Overset component mesh, and (c) Overlapping background and component meshes

4 Numerical validation

The accuracy of the present numerical model is validated using the results of the simulation of flow around a fixed cylinder at Re = 100. Figures 3 and 4 depict the time histories of the drag and lift coefficients, respectively. Fast Fourier Transform (FFT) of the time history of lift coefficient yields to Strouhal number ($St = f_S U/D$) of about 0.169, as depicted in Figure 5.

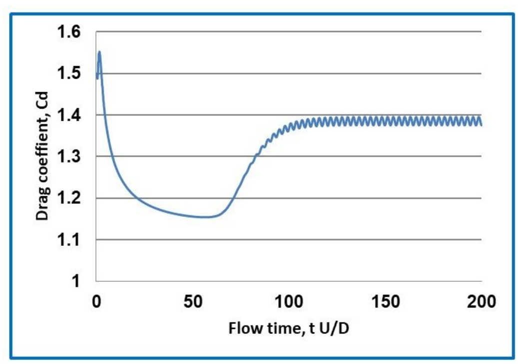

Figure 3: Drag coefficient history of the fixed cylinder at Re = 100

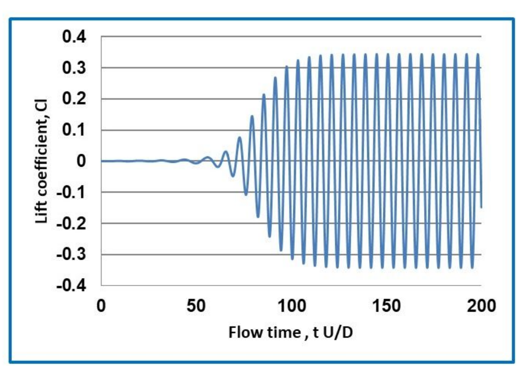

Figure 4: Lift coefficient history of the fixed cylinder at Re = 100

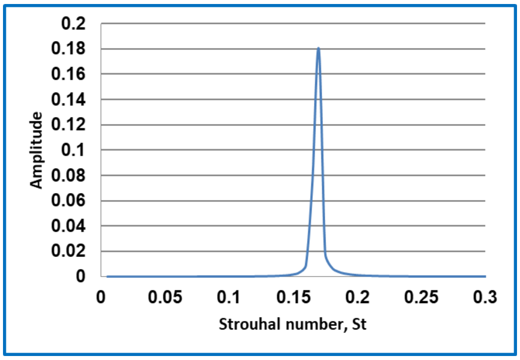

Figure 5: Strouhal number of the fixed cylinder at Re = 100

The computed mean drag coefficient, CD, lift coefficient amplitude, CL, and Strouhal number, St, were compared with the available results reported in the literature. Table 1 depicts an acceptable agreement between the present results and published data.

Table 1: Results comparison of a fixed cylinder at Re = 100

Reference	Cl, max	Cd, mean	St
Placzek *et al.* [16]	0.330	1.370	0.169
Munday and Taira [19]	0.328	1.345	0.165
Westbrook-Netherton [21]	0.354	1.373	0.171
Present study	0.339	1.375	0.169

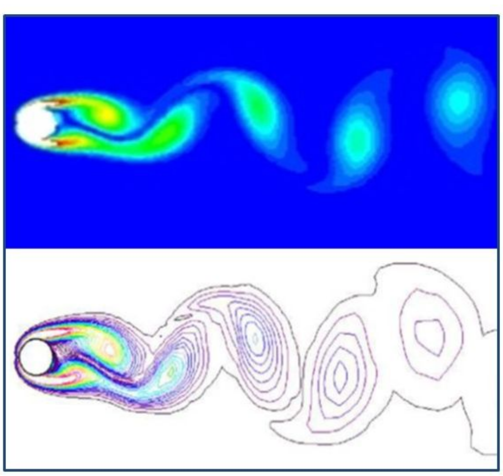

Figure 6: Comparison of instantaneous vorticity field at Re = 100 between the present work (top) and the work presented by Placzek *et al.* [16] (bottom)

Figure 6 depicts the snapshot of the instantaneous vorticity field over the cylinder and its wake. As can be seen, very similar behavior is observed compared with the vorticity contour presented by Placzek *et al.* [16].

5 Results and discussion

In order to assess the capability of the present numerical technique in modeling the flow around a vibrating cylinder, two types of crossflow and inline vibration of a circular cylinder are considered at Re = 100. The simulation setup used for these two types is similar to that for the fixed cylinder, except the cylinder is vibrating now.

5.1 Crossflow vibration cylinder

According to Bishop and Hassan [5], the synchronization or lock-in phenomenon occurs as the forced vibration frequency (f_v) of the cylinder is near the Strouhal shedding frequency (f_s) of the fixed cylinder, i.e., the cylinder and its wake together oscillates at the forced vibration frequency (f_v) of the cylinder, and the Strouhal shedding frequency disappears. On the other hand, outside the lock-in zone, vortices are shed at the Strouhal shedding frequency of the fixed cylinder. Hence, The forces acting on the cylinder are a complex combination of shedding and cylinder motion effects.

In order to examine the capability of the present technique in identifying whether the flow is synchronized or not, simulations are conducted for a cylinder vibrating transversely to the free stream at a frequency $f_v = 0.5 f_s$ (no lock-in) and $f_v = f_s$ (lock-in). The vibration of the cylinder is defined by setting the parallel motion as $X(t) = 0$ and the transverse motion as $Y(t) = A_Y \sin(2\pi f_v t)$, where the oscillation amplitude is $A_Y = 0.25D$.

The lock-in phenomenon is examined by spectral analysis of the lift coefficient time history. When lock-in does not occur ($f_v = 0.5 f_s$), a beating behavior is seen in the time history of the lift coefficient (Figure 7), and two peaks can be observed in the frequency spectrum diagram (Figure 8), where peak 1 corresponds to the cylinder vibration frequency, and peak 2 corresponds to the Strouhal frequency of fixed cylinder. Because of the beating behavior, the arrangement of vortices in the wake is irregular, as shown in Figure 9.

In the case of lock-in occurs ($f_v = f_s$), the beating behavior disappears, and the time history of the lift coefficient is purely sinusoidal (Figure 10), which means only one peak must be present in the frequency spectrum corresponding

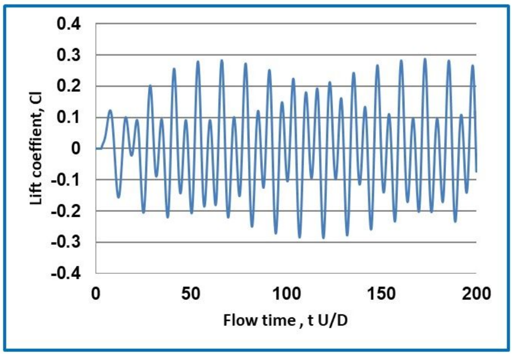

Figure 7: Lift coefficient history at $f_v = 0.5f_s$, crossflow vibration

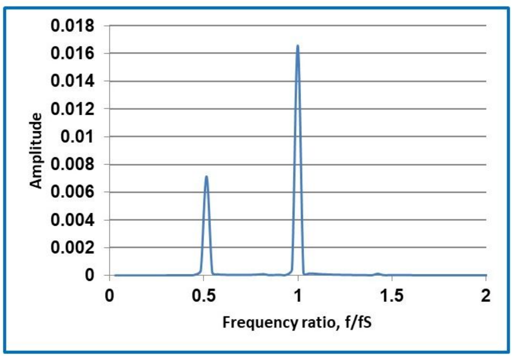

Figure 8: Power spectrum of lift coefficient history at $f_v = 0.5f_s$, crossflow vibration

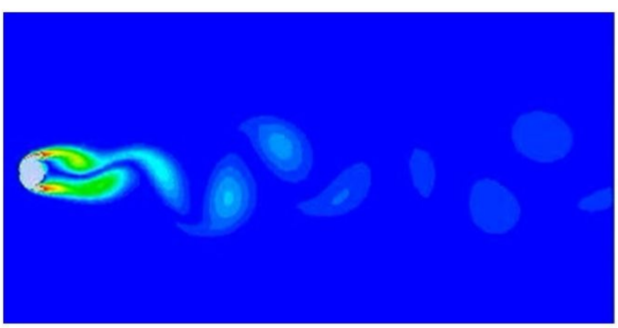

Figure 9: Instantaneous vorticity field at $f_v = 0.5f_s$, crossflow vibration

to the cylinder vibration frequency (Figure 11). Hence, vortices in the wake are arranged in a regular manner as a result of synchronization between the vortex shedding and cylinder motion, see Figure 12. In general, these simulation results are consistent with the previous studies in the literature, demonstrating the efficiency and accuracy of the present technique for modeling flows around the structural system with crossflow vibration.

Phase portrait of lift coefficient against non-dimensional cylinder motion (Y/D) is another graphical representation to identify the lock-in phenomenon. Phase

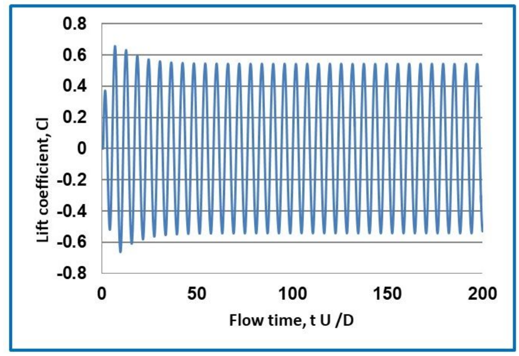

Figure 10: Lift coefficient history at $f_v = f_s$, crossflow vibration

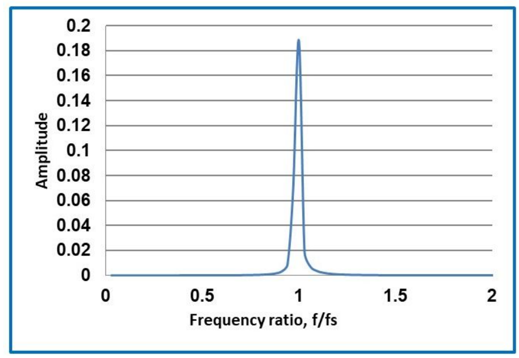

Figure 11: Power spectrum of lift coefficient history at $f_v = f_s$, crossflow vibration

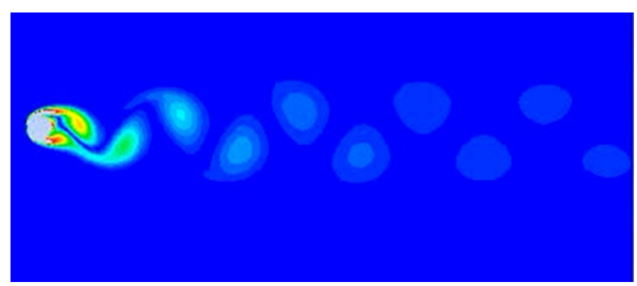

Figure 12: Instantaneous vorticity field at $f_v = f_s$, crossflow vibration

portrait is defined as a complementary tool to power spectrum analysis [16]. Figure 13 shows the phase portrait for the case of no lock-in ($f_v = 0.5f_s$). Chaotic and multiple trajectories are noticed in the phase portrait, which indicates that lift time history is of multiple frequency contents. On the other hand, it can be seen from Figure 14 that the phase portrait for the case of lock-in ($f_v = f_s$) is dramatically different from that of no lock-in. The existence of a unique ovoid shape results from the presence of a single frequency in the lift coefficient response.

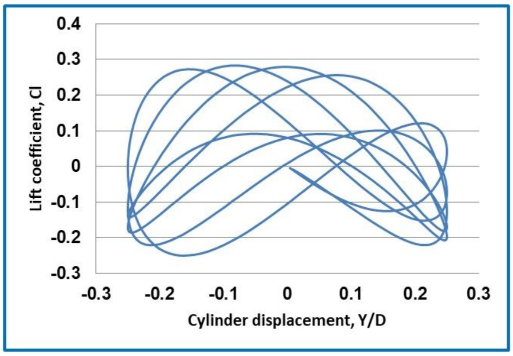

Figure 13: Phase portrait at $f_v = 0.5f_s$, crossflow vibration

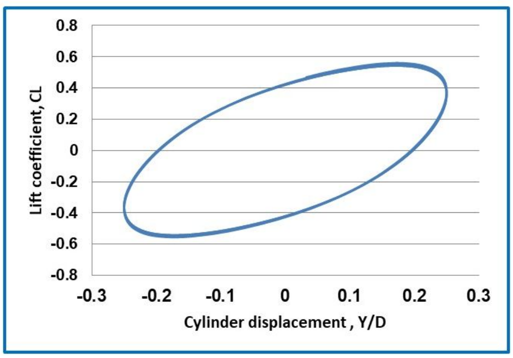

Figure 14: Phase portrait at $f_v = f_s$, crossflow vibration

5.2 Inline vibration cylinder

For inline oscillation, lock-in occurs when the cylinder oscillation frequency is twice the Strouhal vortex frequency of the fixed cylinder, according to Griffin and Ramberg [7] and Hurlbut *et al.* [13]. Simulation is performed for a cylinder vibrating in the parallel direction at frequency two times the Strouhal vortex frequency for the fixed cylinder, i.e. $f_v = 2f_s$. The vibration of the cylinder is defined by setting the transverse motion as $Y(t) = 0$ and the parallel motion as $X(t) = A_X \sin(2\pi f_v t)$, where the oscillation amplitude is $A_X = 0.14D$. Figures 15 and 16 depict the drag and lift coefficients time histories, respectively. This flow has also been numerically investigated by Hurlbut *et al.* [13] and Su *et al.* [15], where the results are used to validate the accuracy of the present numerical overset mesh approach.

Table 2 depicts that the results of this study are consistent with the results of references [13] and [15], respectively. Furthermore, it can be observed that both the lift and drag coefficients increase significantly in comparison with the case of the fixed cylinder.

Figure 17 depicts the power spectral analysis of the lift coefficient during lock-in for the case of inline vibration. Two dominant frequencies can be seen in the spectrum diagram. The first peak is at $f_v/2$, and the second peak is at

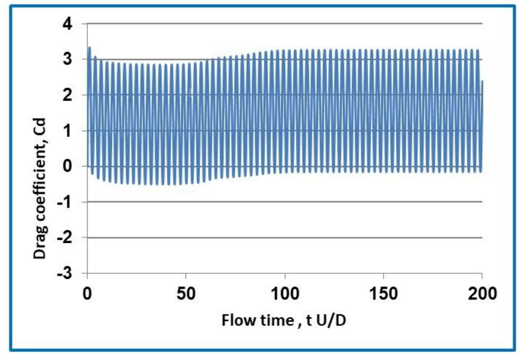

Figure 15: Drag coefficient history at $f_v = 2f_s$, inline flow vibration

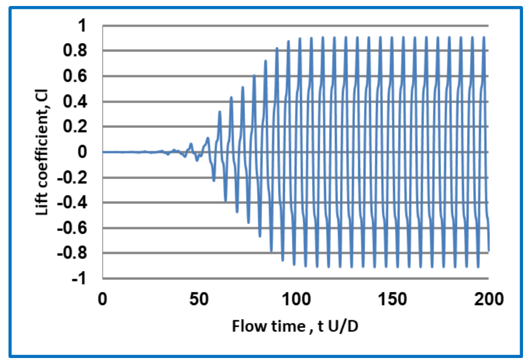

Figure 16: Lift coefficient history at $f_v = 2f_s$, inline flow vibration

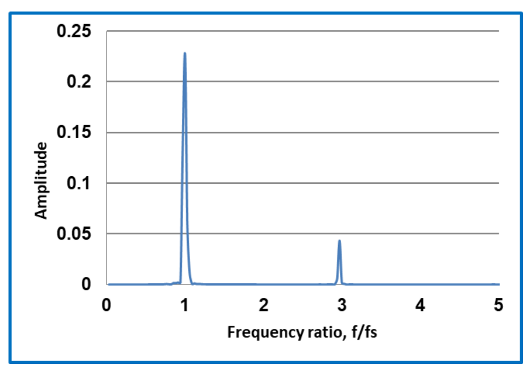

Figure 17: Power spectrum of lift coefficient history at $f_v = 2f_s$, inline flow vibration

Table 2: The comparisons of the inline vibrating cylinder at $f_v = 2f_s$, Re = 100

Reference	Cl, $_{max}$	Cd, $_{mean}$
Hurlbut *et al.* [13]	0.95	1.68
Su *et al.* [15]	0.97	1.70
Present study	0.921	1.692

$3f_v/2$. This predominance of the first plus third harmonics during lock-in agrees with Hurlbut *et al.* [13].

6 Conclusion

In this paper, the dynamic overset mesh technique available in ANSYS FLUENT is proposed to investigate the lock-in phenomenon. The numerical simulation is performed for a circular cylinder vibrating in uniform flow at Re = 100. The technique is verified by considering two test cases: crossflow oscillations and inline oscillations. For the crossflow vibration, the cylinder response is studied for frequency ratios $F = f_V/f_S = 0.5$ and 1. It is observed that lock-in occurs as the cylinder oscillation frequency is near the Strouhal frequency of the fixed cylinder (F = 1), and the aerodynamic coefficients' time history is characterized by a pure sinusoidal response. Nevertheless, The lock-in disappears as the cylinder frequency oscillation shifts away from the Strouhal frequency of the fixed cylinder (F = 0.5), where the aerodynamic coefficients' time history are no longer purely sinusoidal, and a beating behavior is observed. Furthermore, for the inline vibration, lock-in occurs near twice the Strouhal frequency of the fixed cylinder.

On the other hand, in the case of crossflow oscillation, the frequency content in the aerodynamic coefficients' time history is successfully linked to the phase portraits' shape and the vorticity field. A good agreement with previously available data is achieved, which indicates the capability of the present overset mesh technique in solving flows with vibrating solid structure. For future work, different turbulent models could be included to assess the validity of the current approach in solving turbulent flow.

Funding information: The authors state no funding is involved.

Conflicts of Interest: The authors declare no conflict of interest.

Author Contributions: Farouk contributed to methodology, software, and writing the first draft; Alaa contributed to final paper writing, editing, and paper submission; Enass contributed to results analysis and discussion.

References

[1] Baarholm GS, Martin Larsen C, Lie H. Reduction of VIV using suppression devices-An empirical approach. Mar Struct. 2005; 18(7–8):489–510.
[2] Mohammed MJ, Darus IZM. Active Vortex Induced Vibration Controller and neuro identification for marine risers. J Theor Appl Inf Technol. 2014; 70(1):153–62.
[3] Mohammed MJ, Darus IZM. Fuzzy-PID controller on ANFIS, NN-NARX and NN-NAR system identification models for cylinder vortex induced vibration. J Vibroeng. 1410;16(7):3184–96.
[4] Mohammed MJ, Mat Darus IZ. PID controller for NARX and ANFIS models of marine pipe cylinder undergoes vortex induced vibration. J Theor Appl Inf Technol. 2014; 66(1):359–67.
[5] Bishop RE, Hassan AY. The lift and drag forces on a circular cylinder oscillating in a flowing fluid. Proc R Soc A: Math Phys Sci. 1964; 277(1368):51–75.
[6] Koopmann GH. The vortex wakes of vibrating cylinders at low Reynolds numbers. J Fluid Mech. 1967; 28(3):501–12.
[7] Griffin OM, Ramberg SE. Vortex shedding from a cylinder vibrating in line with an incident uniform flow. J Fluid Mech. 1976; 75(2):257–71.
[8] Williamson CH, Roshko A. Vortex formation in the wake of an oscillating cylinder. J Fluids Struct. 1988; 2(4):355–81.
[9] Moe G, Wu ZJ. The lift force on a cylinder vibrating in a current. J Offshore Mech Arctic Eng. 1990; 112(4):297–303.
[10] Yokoi Y, Kamemoto K. Vortex shedding from an oscillating circular cylinder in a uniform flow. Exp Therm Fluid Sci. 1994; 8(2):121–7.
[11] Morse TL, Williamson CH. Prediction of vortex-induced vibration response by employing controlled motion. J Fluid Mech. 2009; 634:5–39.
[12] Aleman MA, Granlund K. Lock-in of vortex shedding from a cylinder undergoing 2-DoF controlled motions. AIAA Aviation 2020 Forum; 2020 Jun 15-19; Virtual Meeting. AIAA; 2020.
[13] Hurlbut SE, Spaulding ML, White FM. Numerical solution for laminar two dimensional flow about a cylinder oscillating in a uniform stream. J Fluids Eng. 1982; 104(2):214–20.
[14] Nobari MR, Naderan H. A numerical study of flow past a cylinder with cross flow and inline oscillation. Comput Fluids. 2006; 35(4):393–415.
[15] Su SW, Lai MC, Lin CA. An immersed boundary technique for simulating complex flows with rigid boundary. Comput Fluids. 2007; 36(2):313–24.
[16] Placzek A, Sigrist JF, Hamdouni A. Numerical simulation of an oscillating cylinder in a cross-flow at low Reynolds number: forced and free oscillations. Comput Fluids. 2009; 38(1):80–100.
[17] Liao CC, Chang YW, Lin CA, McDonough JM. Simulating flows with moving rigid boundary using immersed-boundary method. Comput Fluids. 2010; 39(1):152–67.
[18] Kim S, Wilson PA, Chen ZM. Numerical simulation of force and wake mode of an oscillating cylinder. J Fluids Structures. 2014; 44:216–25.
[19] Munday PM, Taira K. On the lock-on of vortex shedding to oscillatory actuation around a circular cylinder. Phys Fluids. 2013; 25(1):013601.
[20] Kim KH, Choi J. Il. Lock-in regions of laminar flows over a streamwise oscillating circular cylinder. J Fluid Mech. 2019; 858:315–51.
[21] Westbrook-Netherton O. Vortex-Induced Vibration Suppression on a Oscillatory Cylinder [dissertation]. London: Imperial College London; 2015.
[22] Al-Azawy MG, Turan A, Revell A. An Overset mesh approach for valve closure: An LVAD application. In: Gilbert J, Azhari H, Ali H, Quintão C, Sliwa J, Ruiz C, et al., editors. Proceedings of the 9th International Conference on Biomedical Engineering Science Systems and Technologies (BIOSTEC-2016); 2016 Feb 21-23; Rome, Italy. SCITEPRESS; 2016. p. 145–51.